CONTEMP. PHYS., 1986, VOL. 27, NO. 6, 533–552

Digital fluoroscopy: a new development in medical imaging

K. P. Maher and J. F. Malone,
Department of Medical Physics and Bioengineering,
Federated Dublin Voluntary Hospitals, St. James's Hospital,
Dublin 8, and Department of Physics,
Dublin Institute of Technology, Dublin 8, Ireland

ABSTRACT. Fluoroscopy is an X-ray imaging technique which involves the use of photo-electronic components. Digital fluoroscopy refers to their use when coupled to digital image processors. In this paper, medical fluoroscopy is briefly reviewed and video-image digitization is described. Image processing requirements and image processors available for digital fluoroscopy are discussed in detail. Specific reference is made to an application of digital fluoroscopy in the imaging of blood-vessels. This application involves an image subtraction technique which is referred to as digital subtraction angiography (DSA). A number of DSA images of relevance to the discussion are included.

1. Introduction

Digital image-processing techniques have been applied in astronomy, electron microscopy and medicine for many years (Gonzalez and Wintz 1977). As a result of recent developments in digital electronics, new methods of medical X-ray imaging have emerged. One technique, which is primarily used for imaging blood-vessels, involves interfacing an image processor to X-ray equipment of a type already widely used in hospitals (Kruger *et al.* 1981) The technique is called digital fluoroscopy and both the physical and the technical aspects of this development are described below.

Blood-vessel imaging plays an important role in modern medicine. The most successful X-ray technique involves injection of high atomic number solutions directly into major arteries. These solutions are called 'contrast media' and the technique is referred to as angiography (Johns and Cunningham 1971). In a typical procedure, a contrast medium is injected through narrow-bore tubes, called catheters, which have been passed via incisions in the skin, through various arteries, to relevant arterial regions. A number of X-ray films are taken in rapid succession following injection. The procedures are frequently hazardous and efforts have been made to devise safer alternatives (Riederer 1982). The ability to obtain similar images of arteries using simple injections into veins, for example, would dramatically reduce the hazards (Mistretta *et al.* 1981). However, attempts to achieve this objective have generated sizeable problems for both physics and technology. The difficulties arise from a number of factors, which include the dilution of the contrast medium in the blood on its way to the arteries of interest, the intensity and spectral properties of the X-ray beams and the capabilities of the imaging systems (Riederer 1982).

Improvements in the imaging system can be made by using image-subtraction techniques (Mistretta 1974). One method involves photographically subtracting an X-ray film of a region of the body taken before contrast medium is injected, from a film of the same region taken shortly after injection. Ideally, the resulting subtracted film only shows the contrast medium in the arteries, without interference from surrounding bone

and tissue. Recent developments in digital image-processing have included the capability of digitally subtracting images acquired at fine resolutions and high speeds (Harrington *et al.* 1982). The value of such subtracted images is improved by contrast enhancement and various types of spatial and temporal filtration. This technique of digital subtraction angiography is now used routinely in many hospitals following its initial development in Europe (Brennecke *et al.* 1977) and the U.S.A. (Frost *et al.* 1977, Kruger *et al.* 1978). The most common approach involves the use of fluoroscopic imaging-systems interfaced to digital image-processors (figure 1 (*a*)). This paper opens with brief reviews of fluoroscopy (section 2) and image digitization and storage (section 3). Each of the digital image-processing operations required to produce a useful image is discussed in section 4. Types of digital image-processor suitable for digital fluoroscopy are described in section 5. In addition to the references cited in this paper, the reader is also referred to text books by Kruger and Riederer (1984) and Brody (1984) and to conference proceedings edited by Brody (1981), Mistretta *et al.* (1982), Price *et al.* (1982) and Harrison and Isherwood (1984).

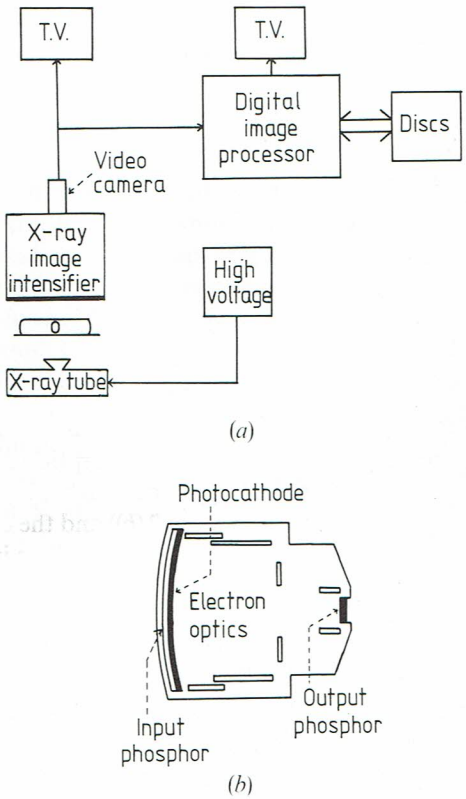

Figure 1. Diagrams of (*a*) a digital fluoroscopy system, and (*b*) an X-ray image intensifier tube.

2. Fluoroscopy

Conventional medical X-ray imaging is essentially a shadow-recording technique; that is, it involves detection of shadows cast by irradiated structures in the body (Johns and Cunningham 1971). In general, two methods of image transduction are employed,

which are referred to as radiography and fluoroscopy. In radiography single X-ray exposures are used and the transducer is generally a light-sensitive film sandwiched between two fluorescent screens. In fluoroscopy continuous X-ray exposures are used and an X-Ray Image Intensifier (XII) viewed by a closed-circuit TV system provides the image transduction (figure 1). This results in a continuous image display with less intense exposure but a lower spatial-resolution as compared to radiography.

The interested reader is referred to Thompson (1978) for a technical account of conventional X-ray imaging. The pertinent aspects of the fluoroscopic technique, which are briefly described below, are X-ray generation, interaction with the patient and transduction of the image.

2.1. *X-ray generation*

The X-ray tube is well known in physics. Medical X-ray tubes use peak accelerating voltages in the range 40–150 kV and currents of up to 1300 mA for single exposures and up to 2 mA for continuous exposures. Tungsten anodes are most commonly used to produce X-ray energy spectra up to 150 keV. As photons less than 30 keV do not contribute to image formation, thin layers of aluminium filter them from the beam to reduce unnecessary patient exposure. Beam size is controlled by using adjustable diaphragms at the output of the X-ray tube.

2.2. *Interaction with the patient*

The modification of energy spectra on passing through the body is due primarily to photoelectric and Compton events and to coherent scattering (Yaffe and Johns 1983). The mass attenuation coefficients of bone, fat, iodine and lead as a function of X-ray energy are shown in figure 2 (*a*). The atomic number dependence of the photoelectric effect results in bone providing more absorption than tissue, hence the general appearance of the familiar chest X-ray film (Johns and Cunningham 1971).

The photoelectric effect is frequently exploited in fluoroscopy through administration of high atomic number solutions to patients so that normally invisible organs can be seen. These 'contrast media' generally provide K-absorption edges in the 30–40 keV range. Commonly used are iodine-based compounds which are injected into the blood stream to radiographically opacify arteries (figure 2 (*b*)) and the chambers of the heart. Barium-based compounds, ingested as in the 'barium meal' or introduced by enema, are used to opacify parts of the alimentary canal.

Emergent X-ray beams contain both primary and scattered radiation. The scattered component reduces the inherent contrast in the beam and may be up to several times the intensity of the primary component. It can be reduced however by using a collimating grid in front of the transducer (Johns and Cunningham 1971). This consists of a series of thin strips of tungsten, for example, aligned in the direction of the primary radiation. Although more sophisticated methods of scatter reduction have been developed (Yaffe and Johns 1983) grids are the most widely used.

2.3. *Image Transduction*

Most X-ray image-intensifiers produce an output image which may be viewed by a video camera (Johns and Cunningham 1971). They differ from conventional image-intensifiers in that a fluorescent screen in intimate contact with the photocathode is used (figure 1 (*b*)). X-ray absorption by the fluorescent screen (i.e. the input phosphor)

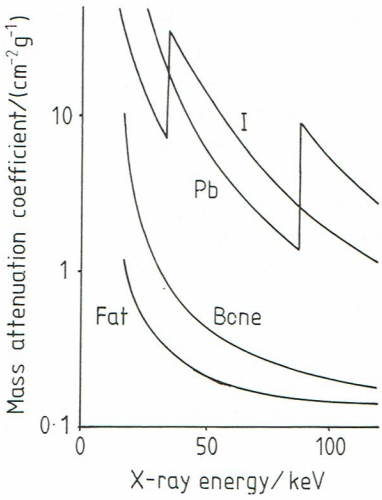

(*a*)

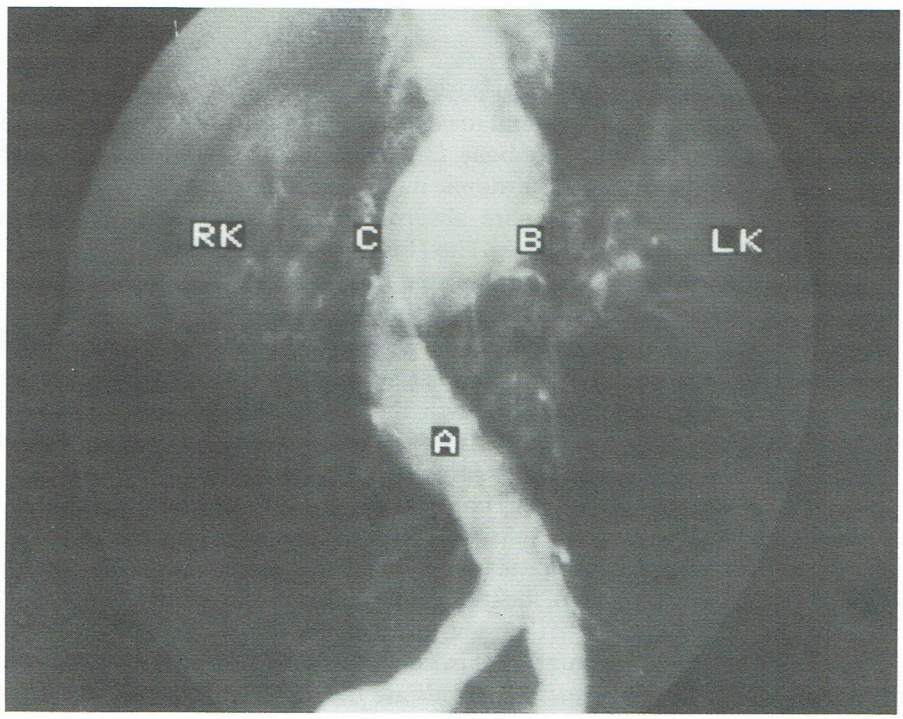

(*b*)

Figure 2. (*a*) Mass attenuation coefficients for iodine, lead, bone and fat as a function of X-ray energy. (*b*) Conventional angiography—image of the abdomen following injection of contrast medium through a catheter (the tip of which is at C) positioned in the aneurysm or abnormal bulge (B) in the aorta (A). Right (RK) and left (LK) kidneys are also seen. A film/screen combination was used with a 70 kV, 320 mA, 250 ms exposure.

results in emission of light which is detected by the photocathode. Caesium iodide forms the input phosphor in modern intensifiers (caesium and iodine having K-edges at 35·98 and 33·17 keV, respectively). The entrance field is typically 15–40 cm in diameter although new generations of intensifier are emerging with larger field sizes. Photoelectrons produced by the input phosphor/photocathode combination are accelerated by 25–35 kV and focused onto the output phosphor by a number of electrodes. An intensified image is produced at the output phospor due to electron acceleration and image minification. The output image is typically 15–35 mm in diameter.

The operating principles of the intensifier are discussed by Mistretta (1979). Performance specifications include conversion factor, detective quantum efficiency and spatial resolution (Thompson 1978). Conversion factor, i.e. the ratio of output luminance to input exposure-rate, ranges from 40 to 200 Cd m^{-2} for an exposure rate of $2{\cdot}58 \times 10^{-7}$ C kg^{-1} s^{-1}, depending on the intensifier. In comparison, the luminance of the tungsten filament of an electric lamp is roughly 10^6 Cd m^{-2}. Detective quantum efficiency is defined as the squared ratio of the output to input signal-to-noise ratios and is of the order of 50% at 40 keV for modern intensifiers (Rowlands and Taylor 1983). Spatial resolution is typically four line-pairs per millimetre which is about half that of a film/fluorescent screen combination.

Performance, however, is limited by veiling glare and by image distortion. Veiling glare occurs when light produced in the phosphors at one point spreads to other points (Seibert *et al.* 1981). As a result, light from the bright areas of the image contributes to darker areas and thereby reduces the image contrast. An improvement in recent designs has resulted from the development of dense needle-structure phosphors which guide scintillations on a fibre-optic basis, thereby reducing dispersion. Image distortion, which arises from the electron optics and the curvature of the input phosphor, may produce distortions of up to 10% in the relative sizes of central and peripheral areas of images. In addition, a spatially non-uniform distribution of image brightness is obtained (Malone *et al.* 1985).

A video camera is optically or fibre-optically coupled to the output phosphor. Principles of video techniques are reviewed in Price and James (1982). The table gives performance data for four commonly used camera tubes. The Plumbicon tube possesses useful characteristics such as a low dark-current and a linear response to illuminance. Its low lag, or image persistence, permits examination of fast moving objects, such as the heart. Recent versions of the Plumbicon have been produced which provide signal-to-noise ratios up to 60 dB (Levin *et al.* 1984). In addition, developments in solid-state imaging detectors, such as charge-coupled and charge-injection devices, have produced cameras of increasing resolution. Their application to fluoroscopy, however, has yet to be investigated.

Performance data for four video camera tubes. (Adapted from Roehrig *et al.* 1981.)

	Orthicon	Vidicon	Plumbicon	Si-vidicon
Signal current (μA)	10	0·2	0·2	0·2
Dark current (nA)	—	15–20	1	7–15
Lag (%)	2	15–25	1–2	5–8
Linearity (γ)	0·6–1	0·65–0·85	1	1
Signal-to-noice ratio (dB)	35–40	45	45–47	45

The performance of an X-ray image-intensifier/video camera system is limited by the combined signal-to-noise ratio characteristics of the components (Roehrig *et al.* 1981). With modern systems, the dominant noise-source is the pre-amplifier of the video camera (Mistretta *et al.* 1981). Spatial resolution is limited by the video standard used. Most systems conform to 525- or 625-line television standards although higher resolutions, of 1000-lines for instance, are also in use (Thompson 1978).

3. Image digitization and storage

Digitization and subsequent storage of video images is a complex task owing to the large volume of information contained in each image and to the high image-rates (Gonzalez and Wintz 1977). In the last five years the task has become less expensive owing to developments in digital electronics. These developments have resulted in improved image digitization and storage technology that has permitted the implementation of digital fluoroscopy. Techniques currently in use are discussed below.

Image digitization and storage is normally achieved by dividing an image into a rectangular matrix (Price and James 1982). Each picture element in the matrix is referred to as a pixel. The brightness of each pixel is represented by an integer, known as the pixel value, and the range of possible integers is called the grey scale (Gonzalez and Wintz 1977).

It is apparent that little loss in spatial resolution occurs when a 525-line video frame is digitized to a matrix of 512×512 pixels. This matrix size could also be used with 625-line cameras when a number of lines of each digitized frame are discarded prior to storage. For a contrast resolution of roughly 1%, eight bit analog-to-digital conversion is necessary for brightness representation. Currently both 256×256 and 512×512 matrices are routinely used in digital fluoroscopy with contrast resolutions of 8, 9 or 10 bits (Harrington *et al.* 1982). Digitization of a video frame to a $512 \times 512 \times 8$ bit matrix represents the generation of over two million bits of data per image. Therefore a typical frame rate of 25 Hz results in data rates which require analogue-to-digital conversion at relatively high speeds.

3.1. *Analogue-to-digital conversion*

Formerly the digitization of video signals required many discrete components. Analogue-to-digital converters consisting of single integrated-circuits are now available from several sources which provide sampling rates of over 30 million samples per second and resolutions of up to eight bits (Peterson 1979). These devices are generally parallel-type converters consisting of a resistive-divider chain, up to 255 comparators and binary encoding logic. Devices of higher resolution are also available.

The period of a video line is approximately 64 μs, of which a portion is blanked for retracing the scanning beam, for which time it contains no pictorial information. Approximately 52 μs of pictorial data is left per line. The digitization of such a line to 512 elements therefore requires an analogue-to-digital converter (ADC) sampling rate of about 10 MHz. It is well known from sampling theory that when an analogue signal has frequency components less than one-half of the sampling rate, the signal will be preserved following sampling (Gonzalez and Wintz 1977). Hence, it is common practice to filter video signals prior to conversion so as to remove frequencies greater than one-half of the sampling rate of the ADC, i.e. 5 MHz in this case. Timing pulses for the digitization circuitry can be derived from the horizontal and vertical synchronization pulses of the composite video signal. These pulses are used in the address control logic of the image storage medium.

3.2. *Image storage*

Once a video frame is digitized, it must be stored in a suitable digital memory. Such a memory may be obtained by using 16 or 64 kbit dynamic random access memory (RAM) devices (Mengers 1980, Goldberg *et al.* 1983). Therefore, 128 of the lower-capacity devices would be required to store one frame of $512 \times 512 \times 8$ bits. However, since a 16 kbit RAM is not fast enough for a 10 MHz data rate, multiplex techniques are employed for image storage (Mengers 1980). This can be achieved using 16 bit serial-to-parallel registers. Digitized data is clocked into the registers at the sampling rate and then written simultaneously to 16 addresses. Versions of the 64 kbit devices are now available which include on-chip 256 bit shift-registers. A similar technique can be used to read memory contents, so that images may be processed, displayed or transferred to bulk storage media for subsequent retrieval.

Suitable bulk storage is provided by digital tape or disc, or their analogue equivalents (Harrington *et al.* 1982). Although digital storage is ideal for faithfully preserving image data, it has the distinct disadvantage that its real-time (i.e. video frame rate) execution is quite complex and expensive. Analogue video tapes and discs are widely available and are capable of real-time operation. However they generally degrade image information to some extent.

A system that employs digital tape has been developed (Roehrig *et al.* 1981) which can record up to 21 600 frames at a resolution of $512 \times 512 \times 13$ bits in real-time. However, digital tape is limited by its sequential-access characteristic. The alternative form is the digital disc. Winchester discs of 84 Mbyte capacity are available commercially, for example, which can store and randomly access over 300 frames of $512 \times 512 \times 8$ bit resolution at roughly 3·5 frames per second and over 1200 frames of $256 \times 256 \times 8$ bit resolution at 12·5 frames per second. Winchester discs with capacities of up to 480 Mbyte are also commercially available. Parallel combinations of these or other discs can be used for storage and retrieval at higher frame rates. Additionally, a number of digital optical discs have recently been developed with capacities between 0·7 and 2·5 Gbytes. At present however, they are non-erasable and have storage rates in order of magnitude lower than Winchester discs.

4. Digital image processing

Image processing requirements for digital fluoroscopy include both image manipulation and data extraction. Requirements discussed below are those used for digital subtraction angiography although they may also apply to other applications.

A fully processed image is shown in figure 3 (*c*). It results from the subtraction of a mask image (figure 3 (*a*)) of the upper thorax and neck from an identical image containing an intravenously injected contrast medium (figure 3 (*b*)). The contrast medium is barely visible in the latter image. The subtraction image (figure 3 (*c*)) however, shows the opacified arteries without interference from surrounding bone and tissue. The processing required to produce such an image includes image transformation, subtraction, enhancement and noise reduction. A similar image may be produced using the temporal filtration of a sequence of images. Furthermore, quantiative information may be extracted from images on the basis of densitometric and dimensional analysis. The following discussion covers these processes.

4.1. *Image subtraction*

Since software-based subtraction of $512 \times 512 \times 8$ bit images is relatively slow, two semiconductor video-frame memories and digital subtraction circuits are generally

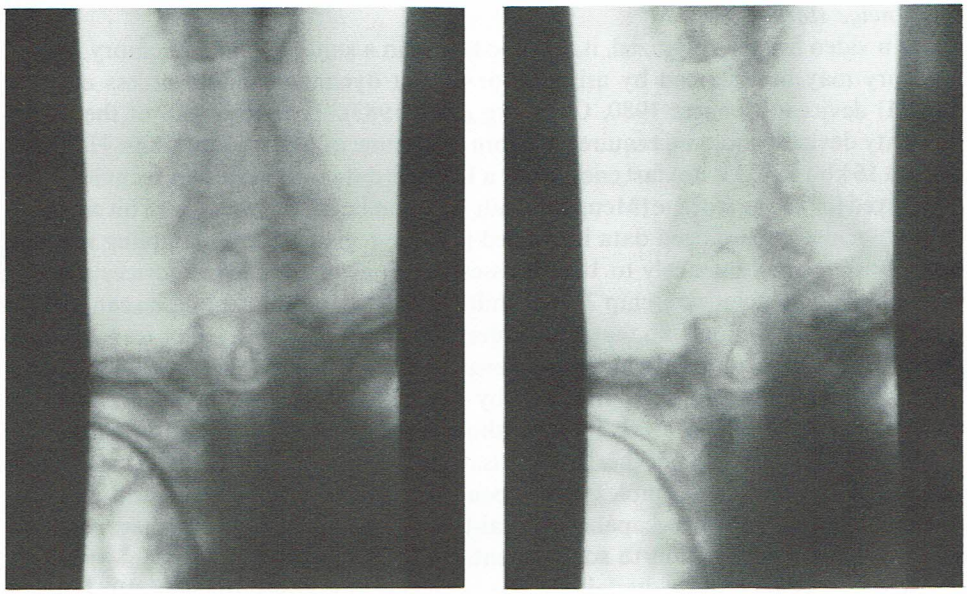

(*a*) (*b*)

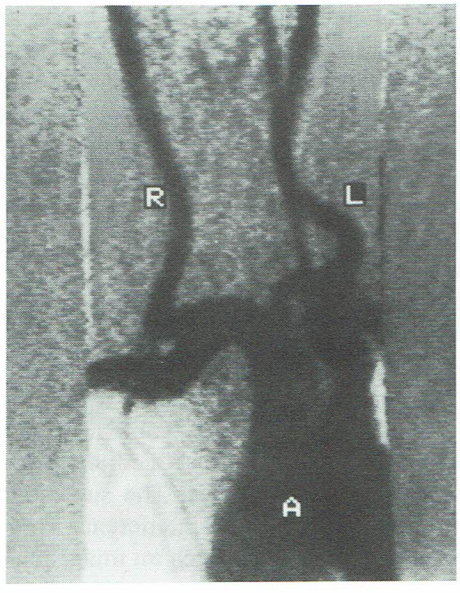

(*c*)

Figure 3. Digital subtraction angiography. (*a*) mask image, (*b*) image containing intravenously injected contrast medium for a patient who had a pulsatile mass in the neck, (*c*) subtraction image showing tortuous arteries corresponding to the pulsatile mass. Right (R) and left (L) carotid arteries and a portion of the aortic arch (A) can be seen. Images were acquired in $256 \times 256 \times 8$ bit matrices using conventional fluoroscopic equipment and a 70 kV, 3 mA continuous exposure.

used (Kruger *et al.* 1978). One memory is used for storing a mask image, acquired just prior to the arrival of contrast medium in the field of view, and the second memory for an image acquired following its arrival. In addition, the second memory can be continuously updated so that a sequence of subtracted images is produced. It is also possible to periodically update the mask image memory so that short-term changes between images can be generated. This technique has been called time-interval-difference imaging (Kruger *et al.* 1979). Another possibility is to use a single memory. The technique here is to acquire a mask image, invert it and to add the result to an image which shows the contrast medium (Mengers 1980).

Subtracted images may be stored in an additional semiconductor memory or fed to digital or analogue storage media. In general, image differences are composed of pixel values which are equal to zero in some regions and are negative in other regions. One method of accommodating this result is to add the midpoint of the grey scale (i.e. a pixel value of 128 for an eight bit memory) to its pixel values (Mengers 1980). The resultant subtraction image thus appears mid-grey with darker-grey levels representing the contrast medium—see, for example, figure 3 (*c*).

Following subtraction of two images acquired directly into memory, the difference between the radiation intensities transmitted through the patient is obtained on a pixel-by-pixel basis. As a result of the quasi-exponential attenuation of X-rays, differences within images are modulated by structures which overlap and underlie opacified arteries. This limitation can be overcome by logarithmically transforming each image before subtraction (Kruger *et al.* 1981).

4.2. *Image transformation*

Images can be logarithmically transformed by using a logarithmic video amplifier, by software techniques or by passing the digitized video data through appropriate look-up-tables (Harrington *et al.* 1982). The analogue approach involves use of circuitry which may, in practice, be affected by instabilities with time and temperature. The second approach is limited by the speed of software execution, which may take times of the order of minutes for a complete image. Transforming digitized images using a look-up-table before semiconductor storage overcomes this speed limitation. However, both digital methods require a contrast resolution which preserves the fidelity of the transformation, i.e. so that sufficient grey levels are assigned to the darker regions of images. A resolution of 10 bits or greater is therefore desirable. It can be shown that following transformation and subtraction, image differences ideally contain contributions solely from the contrast medium (Kruger *et al.* 1981). Such would not be the case without logarithmic transformation. In addition, it can be shown that image differences following the transformation are ideally proportional to the projected thickness of the contrast medium (Nalcioglu *et al.* 1981). This is a value for densitometric purposes, as is discussed later (section 4.7).

4.3. *Image enhancement*

Following subtraction, pixel values can occupy a narrow band of the total available grey scale. As a result, subtraction images may not be suitable for display. This is illustrated by the subtraction image in figure 4 (*a*) of the femoral artery, where the injected contrast medium can almost be seen. A form of image-contrast enhancement is necessary so that this narrow band of pixel values can be transformed to occupy the total grey scale. Figure 4 (*b*) illustrates this process. The femoral artery and its branches are clearly visible following contrast enhancement.

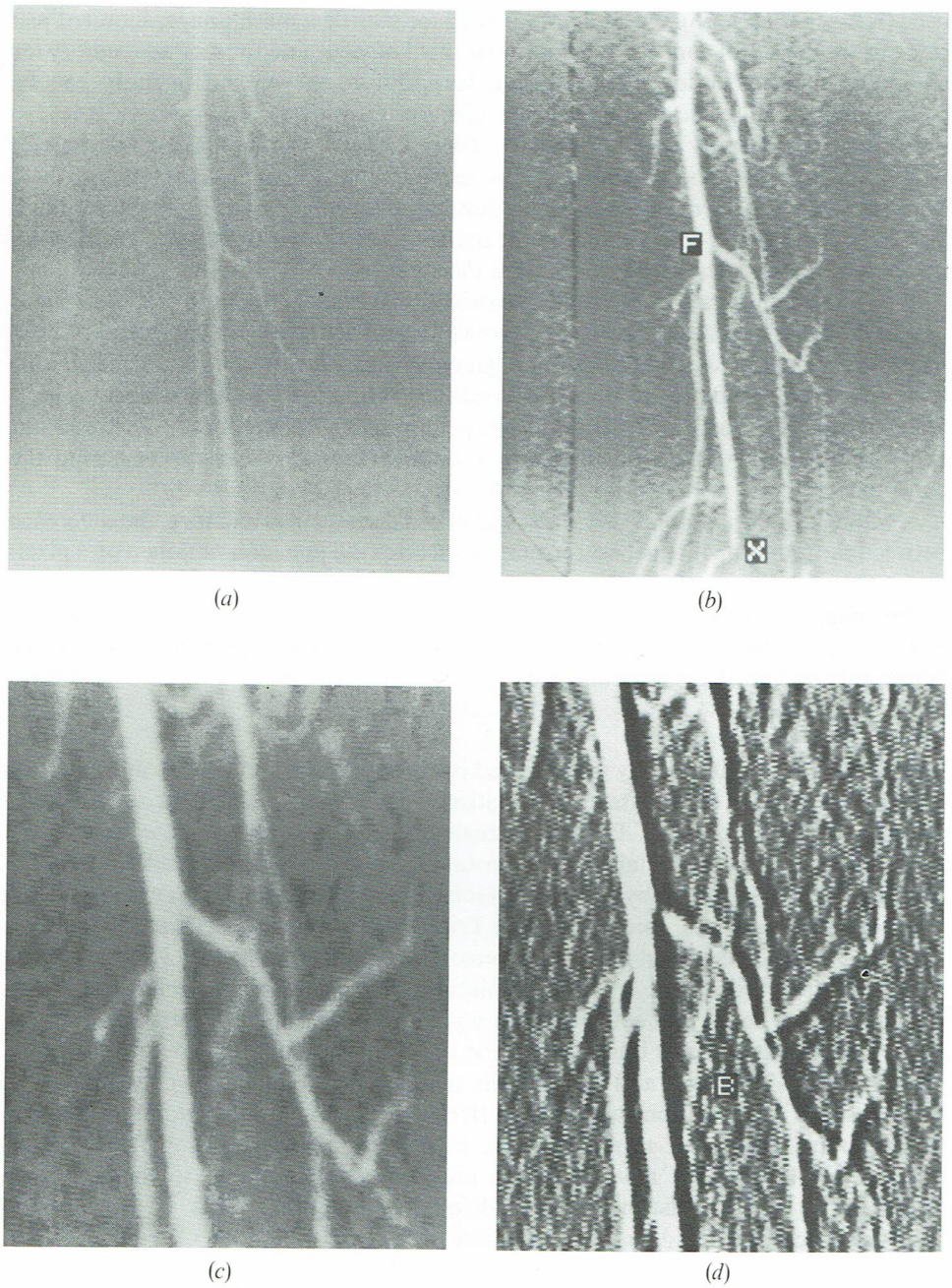

(*a*) (*b*)

(*c*) (*d*)

Figure 4. Image Enhancement. (*a*) subtraction image which has not been enhanced in any form, (*b*) contrast enhanced image obtained from (*a*) using an inverse grey-level window. The femoral artery (F) is now clearly visible and a block in it (at X) is seen. (*c*) smoothed image, (*d*) edge-enhanced image of a magnified view of the central portion of (*b*)—see text for discussion. Image resolutions are $512 \times 512 \times 8$ bit for (*a*) and (*b*), and $256 \times 256 \times 8$ bit for (*c*) and (*d*).

This form of enhancement can be achieved by applying the raw subtracted-image data to variable look-up-tables before digital-to-analogue conversion. As with the logarithmic transformation, these pixel processing operations rescale images in an arithmetic fashion and are image independent. A transformation suitable for digital subtraction angiography is provided by a grey-level window of variable width which may be placed anywhere along the grey scale. Look-up-tables can also be used to generate inverted grey scales. Such an inversion was used for the images in figure 4 and, as a result, the contrast medium appears white on a darker background. Use of normal or inverted grey scales appears to be a matter of personal preference.

Spatial processing operations which are image dependent can be used to smooth or sharpen images (Cocklin *et al.* 1983). These latter operations are illustrated in figure 4 (*c*) and (*d*). It is apparent that some of the detail of figure 4 (*b*) is lost in the smoothed image (figure 4 (*c*)). A more uniform background results however. Edges of arteries are enhanced in figure 4 (*d*) and vessels which are not resolved in figure 4 (*b*) can now be almost discerned, for example, at B. Although these spatial processes have been found to be a value in other fields, for example electron microscopy, they have yet to find routine application in digital subtraction angiography.

4.4. *Image noise reduction*

It is apparent that the detection of differences between images can be limited by the presence of noise. In digital fluoroscopy, image-noise arises from two sources (Kruger *et al.* 1981). The first source is the random nature of X-ray emission which is referred to as quantum noise and follows a Poisson distribution. The second source is called system noise and arises from the imaging components used, for example thermionic emission in the video camera tube, Johnson noise from the load resistor of the camera pre-amplifier and quantization noise from analogue-to-digital conversion. System noise contains contributions which are governed by both Binomial and Poisson distributions (Roehrig *et al.* 1981). It should be noted that noise is increased further in digital subtraction angiography (DSA) since image-variances add on subtraction (Cohen *et al.* 1982). However, the signal-to-noise ratio of images will increase as X-ray exposure is increased and as higher quality imaging components are used. It is also possible to increase it by using digital noise-reduction techniques (Mengers 1980).

As a result of these possibilities, two distinct approaches to the reduction of image noise have been taken in DSA. The first involves pulsing the X-ray tube at high currents, for example 200–1000 mA, and using video cameras of high signal-to-noise ratio (Ovitt *et al.* 1980). The second approach uses standard fluoroscopic equipment, producing lower continuous exposures, for example, 1–10 mA, and digital electronic-noise-reduction (Mengers 1980). This latter method is illustrated in figure 5. A noisy subtraction image (figure 5 (*a*)) results when two single-images are subtracted, which have been acquired using a low exposure and a video camera with a moderate signal-to-noise ratio. Noise can be reduced however by averaging a number of such images before subtraction so that a better image is produced (figure 5 (*b*)).

Pulsed exposure systems use low repetition rates, for example 1–3 Hz, and require interface circuitry between the X-ray generator and the digital image processor—as well as for the video camera interface (Harrington *et al.* 1982). Continuous-exposure systems, on the other hand, operate at standard video frame rates, for example 25 Hz, do not require an X-ray generator interface, and are ideal for imaging fast moving events.

(*a*)

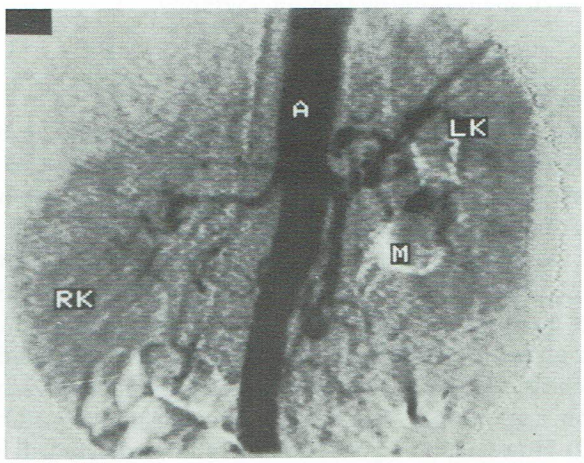

(*b*)

Figure 5. Image Noise Reduction. (*a*) subtraction image obtained from a single mask image and a single image containing contrast medium. An exposure of 75 kV, 2 mA was used with a conventional fluoroscopic system which had a video camera with a nominal SNR of 46 dB. (*b*) image obtained when a number of such images are reduced in noise before subtraction using the algorithm expressed by equation (1) for $N = 4$. Right (RK) and left (LK) kidneys and the aorta (A) are seen. The feature (M) is due to movement of a gas bubble in the overlying bowel between image acquisitions.

Digital noise reduction can be readily achieved by averaging or integrating a number of video frames, N (Kruger *et al.* 1981). Variance in an averaged image can therefore be reduced by a factor N and the signal-to-noise ratio (SNR) improved by a factor $N^{1/2}$ with either technique. These methods, however, suffer from a consequent increase in the depth of the semiconductor memory required to accommodate the results of integrations and to prevent saturation. Various algorithms which combine portions of stored images with portions of incoming images can also be used (figure

5(*b*)). An example of such an algorithm is

$$P_n(x, y) = \frac{1}{N} I_n(x, y) + \left(1 - \frac{1}{N}\right) P_{n-1}(x, y), \tag{1}$$

where $P_n(x, y)$ represents an image stored in semi-conductor memory during frame n, and $I_n(x, y)$ represents an incoming image from the analogue-to-digital converter during this frame. This recursive algorithm improves the SNR by a factor which theoretically approaches $(2N-1)^{1/2}$ and can be implemented without necessitating an increase in the memory depth (Mengers 1980). It should be noted, however, that the SNR improvement actually obtained with any averaging algorithm is dependent on truncation errors introduced by the digital image processor; see, for example, Malone *et al.* (1985).

4.5. *Motion artefact reduction*

As the patient may move between the acquisition of mask and contrast images, subtracted images can contain artefacts due to this motion. These may seriously degrade an image, but can be reduced by selecting a more appropriate mask image, if this is possible, or by digitally realigning portions of the mask image so that better cancellation is achieved (Harrington *et al.* 1982). Image remasking does not add significantly to the complexity of the image processor. However, image realignment at convenient speeds is a complex operation. The nature of projected body movements that cause problems in practice for example breathing and swallowing, is such that simple shifting of images is seldom of value.

4.6. *Temporal filtration*

This involves the application of processing algorithms which are designed to reduce motion artefacts and image noise (Kruger 1981). It relies on the ability of the algorithms to distinguish vessels containing contrast medium from the background anatomy through knowledge of the variation of the concentration of the contrast medium with time following injection. This variation can be approximated by making use of the recursive algorithm expressed by equation (1) and the technique is referred to as recursive filtration. Knowledge of the actual variation can be used to form a 'matched filter' (Riederer *et al.* 1983).

Certain physiological events, such as cardiac contractions, have high temporal frequencies and stationary anatomy has a temporal frequency of zero. Application of a temporal band-pass filter which responds to slowly changing events only, such as the movement of the contrast medium through an artery, may therefore isolate those events within the desired temporal frequency range. The algorithms involve generation of coefficients which reflect this frequency range, weighting each image by its appropriate coefficient and integration of the weighted images (figure 6). This integration provides image noise reduction. It should be noted that it is possible to view these algorithms and image subtractions as temporal-filtration techniques which use different weighting coefficients (Riederer *et al.* 1983).

4.7. *Quantification*

Possibilities arise with digital storage for accessing image data using software techniques. As a result, image differences can be numerically determined from which projected thicknesses of the contrast medium may be inferred (Nalcioglu *et al.* 1981). The extraction of such quantitative information from DSA images is likely to find

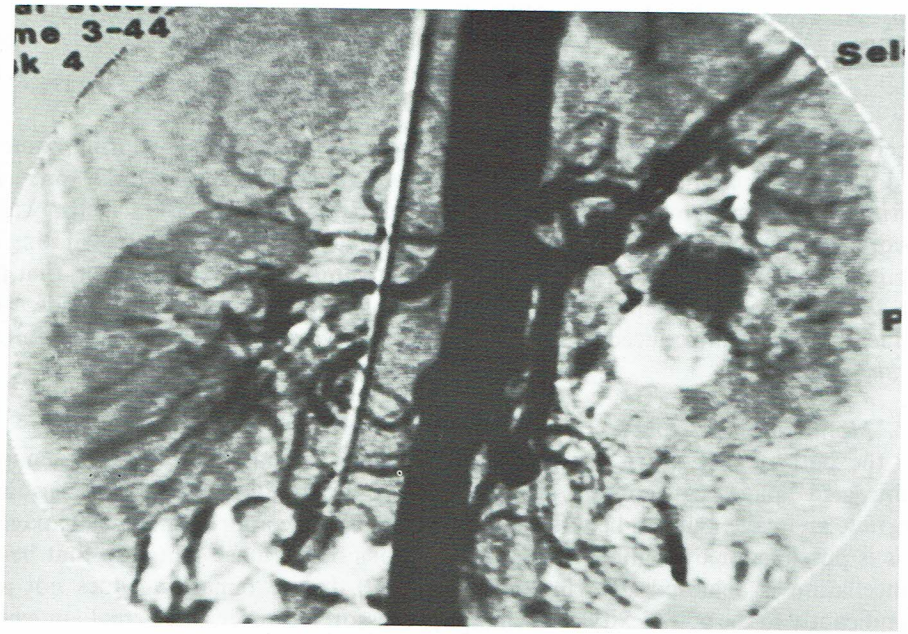

Figure 6. Image obtained by applying a matched temporal filter to the image sequence used for images in figure 5. Filter coefficients were determined using data generated with a region of interest over the aorta.

application (Shaw *et al.* 1982). As discussed earlier, logarithmic transformation is ideally required so that image differences are directly proportional to the thickness of the projected contrast medium. However, in actual imaging, processes such as X-ray scatter and veiling glare contribute to the final image. As a result, the proportionality feature of the transform is lost. So correction techniques must be developed and employed for such quantification. On the assumption that scattered radiation contributes a low-pass spatially-filtered version of the primary radiation, attempts have been made (Shaw *et al.* 1982) to reduce scatter effects through deconvolution of images with approximate inverse-filters. Techniques for reducing veiling glare contributions have been proposed (Seibert *et al.* 1981) by deconvolution of images with inverse point-spread functions. Furthermore, scatter and glare components in images can be estimated by using lead absorbers to derive corrections before logarithmic transformation is performed. Such a technique can establish linear relationships between the image difference and the projected thickness (Maher *et al.* 1985).

The computer generation of curves which represent the variation of the contrast medium concentration with time in a sequence of images can be obtained by this method of quantification (Shaw *et al.* 1982). An example is shown in figure 7. Two regions have been defined around each kidney in an image (figure 7 (*a*)) taken from the same sequence as the images in figure 5. Mean pixel values for each region are computed for images in the sequence. Results are shown against time (figure 7 (*b*)). However, the extent to which this technique will find application in practice has yet to be determined. In addition, area measurements can be made using digital data. These measurements may aid in organ volume estimations—see, for example, Tobis *et al.* (1982).

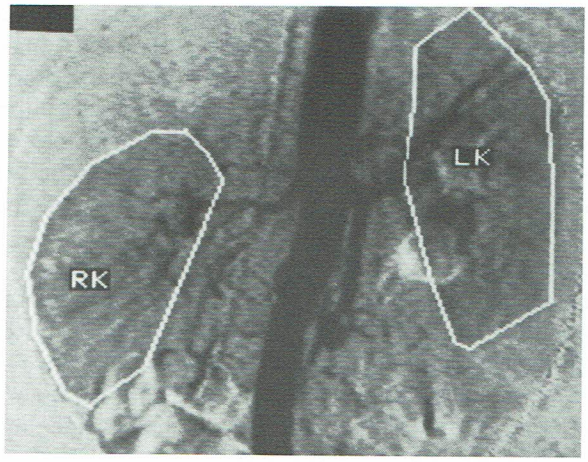

(*a*)

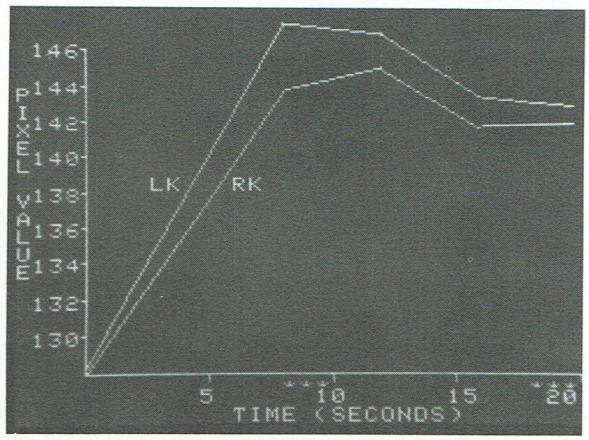

(*b*)

Figure 7. (*a*) Regions for analysis are defined over each kidney (RK, LK) in an image taken from a 20 s sequence. (*b*) plot of mean pixel value against time for the two regions. Pixel values are subtracted from 256, to aid interpretation. An increase in projected thickness is seen as the contrast medium enters each kidney. The curves begin to fall at roughly 10 s, as the contrast medium leaves the kidneys via the renal veins.

The above discussion indicates that complex image processing is not required for DSA. However, routine implementation of the techniques requires sophisticated digital image-processors because of the large amounts of data and the high data rates that were specified in section 3.

5. Image processing systems

Initially, two general types of digital image-processors were developed for digital fluoroscopy. One design consisted of a hard-wired, non-programmable system that could manipulate images at high speeds (Kruger *et al.* 1978). A second design consisted of a more complex computer-based system, which was capable of being programmed but which operated at slower rates (Roehrig *et al.* 1981). In 1980, major commercial

interest in DSA started and since then, most radiological companies have developed at least one design. Available products are quite expensive and range from complete systems, which include both the X-ray system and the image processor, to add-on processors, which can be interfaced to existing fluoroscopic equipment. The latter devices include existing medical image-processors, for example nuclear medicine systems, which have been modified for digital fluoroscopy. Currently available digital image-processors fall basically into three categories and are described below.

5.1. *Real-time systems*

This form of image processing utilizes digital hardware algorithms for real-time (i.e. video frame rate) manipulation of video images (Mengers 1980). Systems are available which typically use eight-bit analogue-to-digital conversion, 512×512 matrix storage with depths up to 16 bits, and microprocessor control. They use high-speed arithmetic units to add, subtract, temporal-filter and contrast-enhance video images. Control is provided using function switches on a control panel. Processed images are converted from digital to analogue form for display or for storage on analogue video tape or disc.

Although these systems provide for real-time processing, their circuitry is fixed and they are not programmable. Furthermore, they do not offer capabilities for deriving quantitative data or for bulk digital-image storage. Nevertheless, the approach has been pursued by a number of radiological companies—see for example Ludvig *et al.* (1982).

5.2. *Minicomputer systems*

These systems utilize a video analogue-to-digital converter (ADC) and a buffer memory interface to a minicomputer (Roehrig *et al.* 1981). Capabilities include image addition, subtraction, contrast enhancement, spatial and temporal filtration, and extraction of quantitative data, at resolutions similar to those of real-time systems. In this category are included nuclear medicine image processors in which the conventional gamma camera interface is replaced by a video ADC (O'Connor *et al.* 1984). Although these systems are widely available in hospitals they do not, in general, provide the high spatial-resolutions required for digital fluoroscopy, since nuclear images are frequently acquired in 64×64 matrices. Moreover, typical data rates in digital fluoroscopy far exceed those routinely encountered in nuclear medicine, where data rates are generally less than 10 kbits s^{-1}, though they may be as high as 30 kbits s^{-1}. However, these image processors do provide extensive image-processing software and recent models have capabilities for manipulating $256 \times 256 \times 16$ bit images.

Minicomputer systems rely on mass digital storage of raw images and post-storage image processing. Although it is apparent that flexibility is provided in the definition of processing algorithms, delays of the order or minutes are involved in the production of processed images. Nevertheless, in contrast to real-time systems, minicomputers offer quantification facilities as well as the convenience of random-access bulk digital storage.

5.3. *Integrated systems*

Interfacing a real-time processing system to a computer offers the combined capabilities of both systems (Nalcioglu *et al.* 1981). Suitable processors of varying sophistication are currently commercially available. A number of systems are based on at least one $512 \times 512 \times 8$ bit memory and standard mini- or micro-computers. Real-time processing is performed peripherally to the central processing unit. Such a system

was used to produce the images presented in this paper. Furthermore, they may be programmed to implement various forms of image enhancement, to extract quantitative data from images and to permit control over commonly used operations using multi-function key pads. They can also be interfaced to digital tape of disc. Moreover, limitations on storage rates of digital discs may be overcome by averaging sets of digitized images in real-time before storage so that effective frame-rates match available storage rates. Other real-time operations, for example subtraction, can then be carried out using the averaged images.

Systems developed purely for DSA include interfaces to most modern X-ray generators as well as software designed for pulsed-exposure sequencing and for the estimation of clinically useful indices from images. It is apparent that these systems permit the real-time production of processed images, without the time-delays involved in software execution and in bulk storage of unprocessed images.

6. Conclusion

The physical and technical aspects of a new development in medical imaging have been described. With regard to its acceptance as an imaging technique, it is important to note that both the basic imaging system and medical expertise in its application are widely available.

However, the suitability of existing fluoroscopic equipment depends on whether pulsed or continuous exposures are used. As discussed in section 4.4., fluoroscopic images of high signal-to-noise ratio (SNR) are required for pulsed exposure DSA because only two images are used to produce the subtraction image. Intense exposures are therefore required. As a result, a number of consequences for the design of digital fluoroscopy systems can be inferred. Firstly, an X-ray tube and an image intensifier suitable for high exposures are needed. Secondly, a variable aperture at the camera input is required because of the resulting high luminance of the output phosphor and of the possible saturation of video images. Thirdly, a video camera of low noise is necessary (for example an SNR of 60 dB). In some systems, for example, low camera noise is achieved through delayed scanning of the target using a progressive (i.e. non-interlaced) mode (Price and James 1982). Since most cameras which are routinely used in fluoroscopy operate in an interlaced mode, and since SNRs of roughly 45 dB are typical, it is apparent that these cameras are not suitable for the pulsed exposure approach. Finally, since X-ray exposures must occur in synchrony with video camera scanning and digital image-acquisition, an interface from the image processor to the X-ray generator and to the scan-control circuitry of the camera is needed—in addition to the video interface. As a result of these and other considerations, sophisticated and expensive fluoroscopic systems are required when pulsed exposures are used. Existing conventional fluoroscopic systems, on the other hand, can be used for continuous exposure DSA, when digital noise-reduction techniques are used. Images used in this paper were acquired using this approach. Detailed comparisons of the two techniques have yet to be reported although images of similar quality have been obtained in some applications (Riederer *et al.* 1983).

Although digital techniques improve the capabilities of imaging systems so that angiography can be performed more safely, conventional procedures have not been totally replaced (Riederer and Kruger 1983). This is due to the limitations of DSA which include lower spatial-resolution, in comparison with radiographic film, and artefacts resulting from patient motion which can seriously degrade subtracted images.

Furthermore, the capability of imaging arteries following a simple intravenous injection has not been completely realized in practice. In order to increase the concentration of the contrast medium in arteries, current techniques involve injection through short catheters inserted in veins in the arm (Chilcote *et al.* 1981) or through longer catheters passed through the venous system to veins adjacent to the heart (Crummy *et al.* 1981). This latter technique was used for the images presented here. Injections normally involve use of high pressure pumps so that, for example, 40 ml of contrast medium is administered at a rate of $20\,ml\,s^{-1}$. Many of these procedures are similar in practice to intra-arterial injections and digital fluoroscopy equipment is also finding application in conventional angiography (Brant-Zawadzki *et al.* 1982, Crummy *et al.* 1982). Intravenous injections, however invasive, are nevertheless considered safer than conventional procedures (Mistretta *et al.* 1981). Since major arteries are punctured in conventional angiography, patients are generally admitted to hospital for a number of days for the examination. For DSA on the other hand, risks from intravenous injections are considered low enough for examinations to be performed on an out-patient basis (Chilcote *et al.* 1981). Accordingly, both the patient and the hospital benefit in terms of convenience, reduced hazards and costs but, as noted above, at the expense of spatial resolution. An additional limitation of DSA arises from arteries filling at similar rates following intravenous injection. As a result, overlapping vessels can mask abnormalities in arteries; see for example the arteries between the left kidney and the aorta in figure 5 (*a*). Such problems rarely occur with arterial injections owing to their selective nature.

Many of the imaging techniques presently used in medicine can be performed as out-patient procedures. These techniques are generally regarded as providing complimentary or correlative medical information. Nuclear medicine examinations, for example, commonly provide physiological information about organ function and typically involve simple intravenous injections of roughly 1 ml of radioactive solution. Furthermore, injections are not required for the anatomical information provided by ultrasonic scanning and are not widely used in magnetic resonance imaging to date. At present however, angiography is regarded as the primary technique for providing the required image detail so that patients with arterial disorders may be effectively treated. Although ionizing radiations are used for the procedures, resultant risks are considered to be low in comparison to the risks arising from a lack of information regarding the disorders.

The clinical acceptance of DSA has not been dependent on reducing radiation exposure, although the potential for dose reduction is evident. A comparison of the radiation doses from pulsed exposure DSA and from conventional angiography, of arteries of the neck, found a ten- to twenty-fold dose reduction using the new technique (Pavlicek *et al.* 1982). Moreover, it is anticipated that techniques such as the temporal filtration of a sequence of images will be found to be up to six times more dose efficient than the subtraction of two images only, as occurs in pulsed exposure DSA (Riederer *et al.* 1983). However, comparisons of doses from conventional techniques with those from both continuous and pulsed exposure DSA have yet to be widely reported.

Digital subtraction angiography is the first application of digital techniques to fluoroscopy in particular, and to projection radiography in general, to have gained widespread acceptance. Advances in X-ray generation, image transduction and digital image-storage are likely to find application in the whole field of radiology. Rising costs of radiographic film, because of increasing silver prices, indicate that video image-acquisition coupled with digital image-storage and transmission may already be

economically viable (Nudelman *et al.* 1982). Many other medical imaging techniques such as ultrasound, nuclear medicine, computerized tomography and magnetic resonance imaging already generate digital images. It is anticipated that digital fluoroscopy will contribute to this development of digital imaging in medicine. More fundamental developments in image transduction are required however before an absolute rival to film-based radiography is found.

Acknowledgments

We are grateful to Drs G. D. Hurley and D. P. McInerney of the Meath and Adelaide Hospitals, Dublin, for the images used in this paper; to Ms B. Clarke for typing the manuscript; and to Mr J. Nolan for photographic assistance.

References

Brant-Zawadzki, M., Gould, R., Norman, D., Newton, T. H. H., and Lane, B., 1982, *Am. J. Neuroradiology*, **3,** 593.

Brennecke, R., Brown, T. K., Bursch, J., and Heintzen, P., 1977, *Digital Image Processing*, edited by H. H. Nagel (Berlin: Springer-Verlag), pp. 244–262.

Brody, W. R. (editor), 1981, *Digital Radiography* (Bellingham: Society of Photo-Optical Instrumentation Engineers).

Brody, W. R., 1984, *Digital Radiography* (New York: Raven Press).

Chilcote, W. A., Modic, M. T., Pavlicek, W. A., Little, J. R., Furlan, A. J., Duchesneau, P. M., and Weinstein, M. A., 1981, *Radiol.*, **139,** 287.

Cocklin, M. L., Gourlay, A. R., Jackson, P. H., Kaye, G., Kerr, I. H., and Lams, P., 1983, *Image and Vision Computing*, **1,** 67.

Cohen, G., Wagner, L. K., and Rauschkolb, E. N., 1982, *Radiol.*, **144,** 613.

Crummy, A. B., Stieghorst, M. F., Turski, F. A., Strother, C. M., Lieberman, R. P., Sackett, J. F., Turnipseed, W. D., Detmar, D. E., and Mistretta, C. A., 1982, *Radiol.*, **145,** 303.

Crummy, A. B., Strother, C. M., Lieberman, R. P., Stieghorst, M. F., Sackett, J. F., Wojtowycz, M. M., Kruger, R. A., Turnipseed, W. D., Ergun, D. L., Shaw, C. G., Mistretta, C. A., and Ruzicka, F. F., 1981, *Radiol.*, **141,** 33.

Frost, M. M., Fisher, H. D., Nudelman, S., and Roehrig, H., 1977, *Application of Optical Instrumentation in Medicine VI*, edited by J. E. Grey and W. R. Hendee (Bellingham: Society of Photo-Optical Instrumentation Engineers), pp. 208–215.

Goldberg, M., Smith, A. M., and Masters, M., 1983, *Applications of Digital Image Processing*, edited by A. Oosterlinck and A. G. Tescher (Bellingham: Society of Photo-Optical Instrumentation Engineers), pp. 415–424.

Gonzalez, R. C., and Wintz, P., 1977, *Digital Image Processing* (Reading: Addison-Wesley), pp. 21–29.

Harrington, D. P., Boxt, L. M., and Murray, P. D., 1982, *Am. J. Roentgenology*, **139,** 781.

Harrison, R. M., and Isherwood, I. (editors), 1984, *Digital Radiology: Physical and Clinical Aspects* (London: The Hospital Physicists' Association).

Johns, H. E., and Cunningham, J. R., 1971, *The Physics of Radiology* (Springfield: C. C. Thomas), pp. 580–647.

Kruger, R. A., 1981, *Med. Phys.*, **8,** 466.

Kruger, R. A., Mistretta, C. A., Houk, T. L., Riederer, S. J., Shaw, C. G., Goodsitt, M. M., Crummy, A. B., Zwiebel, W., Lancaster, J. C., Rowe, G. G., and Fleming, D., 1979, *Radiol.*, **130,** 49.

Kruger, R. A., Mistretta, C. A., Lancaster, J., Houk, T. L., Goodsitt, M., Shaw, C. G., Riederer, S. J., Hicks, J., Sackett, J., Crummy, A. B., and Fleming, D., 1978, *Opt. Eng.*, **17,** 652.

Kruger, R. A., Mistretta, C. A., and Riederer, S. J., 1981, *IEEE Trans. nucl. Sci.*, **28,** 205.

Kruger, R. A., and Riederer, S. J., 1984, *Basic Concepts of Digital Subtraction Angiography* (Boston: G. K. Hall Medical Publishers).

Levin, D. C., Shapiro, R. M., Boxt, L. M., Dunham, L., Harrington, D. P., and Ergun, D. L., 1984, *Am. J. Roentgenology*, **143,** 447.

LUDVIG, J. W., VERHOEVEN, L. H. J., and ENGELS, P. H. C., 1982, *Br. J. Radiol.*, **55,** 545.
MAHER, K. P., O'CONNOR, M. K., and MALONE, J. F., 1985, *Med. Biol. Engng. Computing*, **23,** Suppl., 1534.
MALONE, J. F., O'CONNOR, M. K., and MAHER, K. P., 1985, *Br. J. Radiol.*, Suppl. No. 18, 39.
MENGERS, P., 1980, *IEEE Trans. nucl. Sci.*, **27,** 1192.
MISTRETTA, C. A., 1974, *Opt. Engng.*, **13,** 134.
MISTRETTA, C. A., 1979, *The Physics of Medical Imaging: Recording System Measurements and Techniques*, edited by A. G. Haus (New York: American Association of Physicists in Medicine), pp. 182–205.
MISTRETTA, C. A., CRUMMY, A. B., and STROTHER, C. M., 1981, *Radiol.*, **139,** 273.
MISTRETTA, C. A., CRUMMY, A. B., STROTHER, C. M., and SACKETT, J. F. (editors), 1982, *Digital Subtraction Arteriography: An Application of Computerized Fluoroscopy* (Chicago: Year Book Medical Publishers).
NALCIOGLU, O., ROECK, W. W., PEARCE, J. G., GILLAN, G. D., and MILNE, E. N. C., 1981, *IEEE Trans. nucl. Sci.*, **28,** 219.
NUDELMAN, S., HEALY, J., and CAPP, M. P., 1982, *Proc. Inst. elect. electron. Engrs.*, **70,** 708.
O'CONNOR, M. K., MOLLOY, M., MAHER, K., and MALONE, J. F., 1984, *Br. J. Radiol.*, **57,** 553.
OVITT, T. W., CRISTENSON, P. C., FISHER, H. D., FROST, M. M., NUDELMAN, S., ROEHRIG, H., and SEELEY, G., 1980, *Am. J. Roentgenology*, **135,** 1141.
PAVLICEK, W., WEINSTEIN, M. A., MODIC, M. T., BUONOCORE, E., and DUCHESNEAU, P. M., 1982, *Radiol.*, **145,** 683.
PETERSON, J. G., 1979, *IEEE J. Solid-St. Circuits*, **14,** 932.
PRICE, R. R., and JAMES, A. E., 1982, *Digital Radiography: A Focus on Clinical Utility*, edited by R. R. Price, F. D. Rollo, W. G. Monahan and A. E. James (New York: Grune and Stratton), pp. 5–50.
PRICE, R. R., ROLLO, F. D., MONAHAN, W. G., and JAMES, A. E. (editors), 1982, *Digital Radiography: A Focus on Clinical Utility* (New York: Grune and Stratton).
RIEDERER, S. J., 1982, *IEEE Trans. Med. Imaging*, **1,** 48.
RIEDERER, S. J., HALL, A. L., MAIER, J. K., PELC, N. J., and ENZMANN, D. R., 1983, *Med. Phys.*, **10,** 209.
RIEDERER, S. J., and KRUGER, R. A., 1983, *Radiol.*, **147,** 633.
ROEHRIG, F., NUDELMAN, S., FISHER, H. D., FROST, M. M., and CAPP, M. P., 1981, *IEEE Trans. nucl. Sci.*, **28,** 190.
ROWLANDS, J. A., and TAYLOR, K. W., 1983, *Med. Phys.*, **10,** 786.
SEIBERT, J. A., NALCIOGLU, O., and ROECK, W. W., 1981, *Digital Radiography*, edited by W. R. Brody (Bellingham: Society of Photo-Optical Instrumentation Engineers), pp. 310–318.
SHAW, C. G., ERGUN, D. L., MYEROWITZ, P. D., VAN LYSEL, M. S., MISTRETTA, C. A., ZARNSTORFF, W. C., and CRUMMY, A. B., 1982, *Radiol.*, **142,** 209.
THOMPSON, T. T., 1978, *A Practical Approach to Modern X-Ray Equipment* (Boston: Little, Brown and Co.).
TOBIS, J., NALCIOGLU, O., JOHNSTON, W. D., SEIBERT, J. A., ISERI, L. T., ROECK, W. W., ELKAYAM, W., and HENRY, W. L., 1982, *Am. Heart J.*, **104,** 20.
YAFFE, M. J., and JOHNS, P. C., 1983, *J. appl. Photogr. Eng.*, **9,** 184.